Pergamon

Bioorganic & Medicinal Chemistry 9 (2001) 2571–2580

BIOORGANIC & MEDICINAL CHEMISTRY

Uptake and Intracellular Transport of RNA Aptamers in African Trypanosomes Suggest Therapeutic "Piggy-Back" Approach

Matthias Homann and H. Ulrich Göringer*

Department of Microbiology and Genetics, Darmstadt University of Technology, Schnittspahnstr. 10, 64287 Darmstadt, Germany

Received 5 October 2000; revised 6 December 2000; accepted 7 December 2000

Abstract—African trypanosomes are protozoan organisms that multiply as extracellular parasites in the blood of humans and other mammals. The parasites escape destruction by the host immune system by periodically changing their glycoprotein surface coat. This phenomenon is known as antigenic variation and is responsible for the inability of the infected host to clear the infection. Previously we reported the selection of RNA aptamers that bind to a 42 kDa surface protein of *Trypanosoma brucei*. The polypeptide is localised within a specific substructure on the parasite surface, the so-called flagellar pocket. Here we analyse the fate of the aptamers upon binding to the flagellar pocket. At elevated temperatures, both terminal ends of the RNAs are degraded to form a stable core structure of approximately 50 nucleotides. The RNAs become rapidly internalised by endocytosis and are transported to the lysosome by vesicular transport. The endocytotic process is sequence specific and does not occur with randomised RNA sequences or significantly shortened aptamer fragments. Co-localisation experiments with transferrin suggest a receptor-mediated uptake. The identified internalisation and transport pathway was used to target aptamer-coupled biotin molecules to the lysosome. This demonstrates that the RNAs can be used as 'piggy-back' molecules to target aptamer-coupled compounds/toxins to the lysosomal compartment of the parasite. © 2001 Published by Elsevier Science Ltd.

Introduction

Some of the most severe parasitic diseases in mammals including humans are caused by protozoan organisms that multiply within the cells and body fluids of the infected hosts. Being exposed to the attack by the host immune system, the parasites have evolved intricate defence strategies to escape recognition and clearance by the humoral as well as the cellular immune response.[1–5] One of the most successful evasion strategies is the intracellular multiplication as exemplified by the invasion and penetration of liver and red blood cells in the case of *plasmodia*,[6] of macrophages in the case of *leishmania*[7] and several phagocytic and non-phagocytic cell types in the case of *Trypanosoma cruzi*.[8] These parasites multiply and differentiate inside the cells and only during short periods of their life cycle, specialised cell types are released into the blood. In the case of *Plasmodium yoelii*, merozoites have adapted to the extracellular environment by expressing variable forms of a receptor molecule, thus avoiding its rapid inactivation by host antibodies.[9]

Only few protozoan parasite species are known to multiply exclusively extracellularly and all of them belong to the group of salivarian (African) trypanosomes. The best-studied representative of that group is *Trypanosoma brucei*, which is transmitted by tsetse flies and causes sleeping sickness in humans as well as in wild and domestic animals. *T. brucei* multiplies in the peripheral blood and lymphatic fluids of its mammalian hosts. Its cell surface is covered with a dense coat of approximately 10^7 copies of a membrane bound glycoprotein termed variant surface glycoprotein (VSG). Several segments of its N-terminal domain are exposed to the extracellular environment and consequently a strong immune response is induced upon infection.[10] However, a few parasite cells evade the immune response by switching to the expression of a different VSG variant, a process termed antigenic variation.[11–13] The parasite can "choose" from at least 1000 different VSG genes in what seems to be a stochastic recombination event

*Corresponding author. Tel.: +49-6151-16-28-55; Fax: +49-6151-16-29-56; e-mail: goringer@hrzpub.tu-darmstadt.de

0968-0896/01/$ - see front matter © 2001 Published by Elsevier Science Ltd.
PII: S0968-0896(01)00032-3

occurring at an estimated frequency of 10^{-2} to 10^{-7} per generation.[14–16] Hence, the high variability of surface structures that are exposed and accessible to the immune system is the cause for the inability of the host to clear the infection.

Aside from the variable characteristics of the VSGs, several invariant features of the trypanosome surface have been identified and may represent potential targets for novel therapeutic strategies. First, VSG molecules themselves contain structurally conserved C-termini.[17–19] Second, invariant surface glycoproteins (ISGs) and transporter and receptor complexes have been identified. Although some of these molecules are distributed over the entire surface, they are inaccessible to the host immune reponse.[20–22] Third, since the dense layer of the VSGs functions as a protective barrier towards larger molecules, trypanosomes have developed a specialised 'organelle-like' surface structure for the regulated passage of nutrients and macromolecules. Endo- and exocytotic processes are restricted to the flagellar pocket (FP), a membrane invagination around the base of the flagellum.[23,24] The FP harbours a number of invariant receptor molecules that regulate the uptake of essential nutrients like purines,[25,26] Fe^{3+}-transferrin complexes[27,28] or high and low-density lipoprotein particles[29,30] (HDL, LDL).

All of the described surface elements are potential targets for an approach that utilises in vitro selected nucleic acids to circumvent the antigenic switch. Nucleic acid aptamers may be selected to recognise either the invariable features of the VSGs or constant protein molecules that are otherwise buried within the VSG layer. Aptamers conjugated to immunogenic tags have the potential to redirect the host immune system to the trypanosome surface despite the repeating changes of the VSG coat. On the other hand, aptamers recognising invariant receptor molecules might be used as carriers to facilitate the uptake of toxic compounds leading to intracellular destruction.

We have previously reported two in vitro selection experiments using live *T. brucei* cells as binding targets.[31] RNA aptamers were isolated that belonged to three families according to primary and secondary structure homologies. Aptamers from the main group share the potential to form a bulged hairpin secondary structure. They are able to penetrate into the flagellar pocket of the parasite and recognise a protein target of 42 kDa. The polypeptide is exclusively expressed in the infective bloodstream stage of the parasite, thus, making it a candidate target for the approach described above.

Here we present a characterisation of one of the most effective aptamers, RNA 2-16. We analyse the stability of the RNA, its optimal length and the processing events after binding to the flagellar pocket on the trypanosome surface. At higher temperatures, bound 2-16 RNA is degraded to a 50 nucleotide core structure, which becomes endocytosed and transported to the lysosome. Co-localisation experiments with transferrin suggest a receptor mediated endocytosis pathway. The results suggest the usage of aptamer 2-16 as a 'piggy-back' delivery molecule to target the lysosomal compartment of trypanosomes. This was verified by directing aptamer-bound biotin molecules to the lysosome.

Results

Stability of bound RNA

To analyse the fate of the RNA aptamers after binding to the 42 kDa protein target within the flagellar pocket, we used radioactively (^{32}P)-labelled aptamer 2-16.[31] 5′- or 3′-end labelled 2-16 RNA was incubated with living MITat 1.4 trypanosomes at 0 °C for 20 min and the cell-bound RNAs were separated from unbound RNAs by repeated washing steps. During all steps the temperature was kept below 4 °C. Only minor RNA degradation was observed under these conditions and $\geq$90 % of the bound RNA remained full length (Fig. 1A). This RNA-cell preparation was either incubated for additional 40 min at 0 °C or shifted to incubation temperatures of 12, 24 or 37 °C. At these temperatures, rapid cleavage of the bound RNAs was observed with only few specific cleavage sites at the very ends of the RNAs (Fig. 1A). The most sensitive hydrolysis positions were −12 and −72 from the 5′-end (Fig. 1A, left panel), corresponding to U12 and G72 (see Fig. 2C for a secondary structure model of aptamer 2-16). Identical sites were found using 5′-end labelled 2-16 RNA (Fig. 1A, right panel). Upon extended incubation at 24 or 37 °C, the 5′ as well as 3′-fragments were degraded to even smaller fragments (Fig. 1A). The half-life ($t_{1/2}$) of trypanosome-bound 2-16 RNA decreased from more than 120 min at 0 °C to about 3 min at 37 °C (Fig. 1B). The predominant cleavage sites correspond to single stranded regions[31] and the lack of hydrolysis in the central portion of aptamer 2-16 is suggestive of an RNase-resistant core structure. Together with our previous results that the RNA is stable during the binding reaction even at higher temperatures,[31] we conclude that only parasite-bound 2-16 RNA is degraded. This finding suggests the presence of a parasite-bound RNase activity proximal to the aptamer binding site within the flagellar pocket.

Determination of a minimal RNA aptamer binding core

The minimal sequence of aptamer 2-16 still capable of interacting with the parasite surface was determined in a boundary experiment. An alkaline hydrolysis ladder was produced from 5′ as well as 3′ radioactively end-labelled 2-16 RNA, and the pools of shortened RNA species were incubated with living MITat 1.4 trypanosomes at 0 °C for 2, 4 and 8 min. Well defined boundaries were identified at positions U64/G65 at the 3′-end and at positions C14/G15 at the 5′-end (Fig. 2A). Both boundaries are located within single stranded regions of the secondary structure model of aptamer 2-16 (Fig. 2C). RNA species that contain at least U64 and G65 bind well to trypanosomes, whereas shorter ones do not

bind at all. At the 5′-end, the single stranded nucleotides up to position C14 can be deleted. To confirm these results we constructed a truncated 2-16 RNA only consisting of a "central core" from G15 to C67. Surprisingly, the binding activity of this aptamer was completely lost ($K_d > 1\,\mu M$). This indicates that full binding activity of the shortened 2-16 RNA variants is retained only in the context of an intact opposite end. To control this effect, a 3′-shortened aptamer including the sequence from G1 to C67 (termed RNA 2-16/67) was synthesised. The RNA was 3′-end labelled and an alkaline hydrolysis ladder was produced for the determination of the 5′-boundary (Fig. 2B, left panel). In the context of the 3′-shortened aptamer, only 4 nucleotides

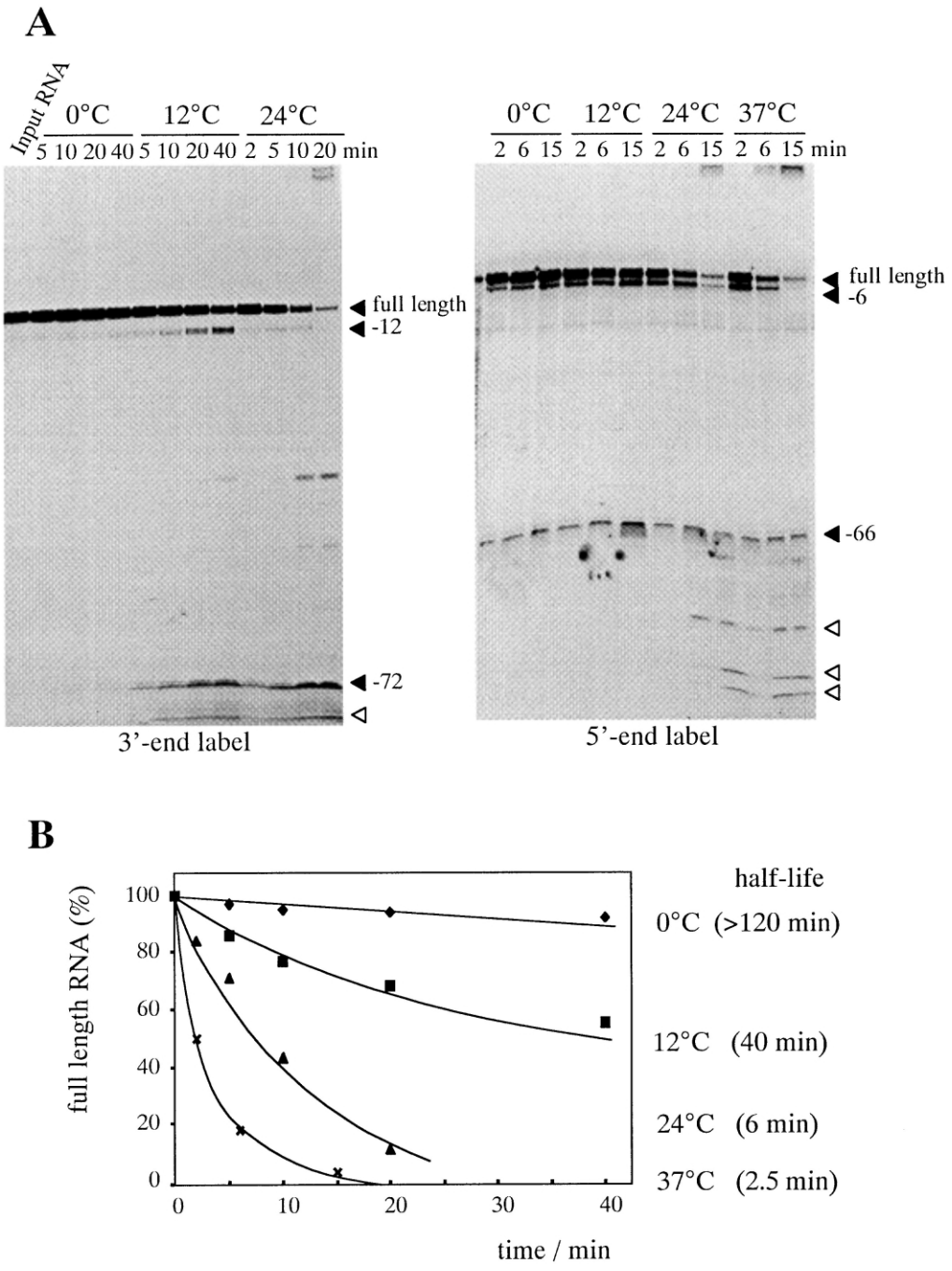

Figure 1. Stability of RNA aptamer 2-16 bound to MITat 1.4 trypanosomes. (A) Gel analysis of the degradation kinetic of (^{32}P) end-labelled 2-16 RNA (left panel: 3′-end labelled aptamer; right panel: 5′-end labelled aptamer). After incubation of the RNA with parasite cells for 20 min at 0 °C, trypanosomes and trypanosome-bound RNA were collected by centrifugation and further incubated at the indicated temperatures for 0 to 40 min. Major cleavage sites are U12 (position −12 in the 3′-labelled RNA which is equivalent to −66 in the 5′-labelled RNA) and G72 (position −72 in the 3′-labelled RNA which corresponds to −6 in the 5′-labelled RNA). Further degradation was observed at higher temperatures (open triangles). (B) Graphical representation of the data derived from a densitometric analysis of the degradation kinetic at 0–24 °C for the 3′-labelled RNA and at 37 °C for the 5′-labelled RNA. Half-lifes ($t_{1/2}$) were determined from 4 independent experiments and identical results were obtained with 3′- or 5′-end labelled RNA. Average half-lifes are indicated next to the graph.

(up to A4) could be removed from the 5′-end without loss of binding activity as compared to 15 nucleotides with the full-length 2-16 RNA.

To identify the shortest aptamer-derived RNA fragment that was still active in binding, the boundary experiment was performed with alkaline hydrolysis ladders from uniformly [α-^{32}P] UTP-labelled 2-16/67 RNA (Fig. 2B, right panel). No fragments shorter than 63 nucleotides were able to bind to the parasite cells. As a control, internally labelled full length aptamer 2-16 was used, and the same result was obtained (data not shown). These results indicate that the 3′-end is already shortened to the minimum length, whereas an additional four nucleotides can be removed from the 5′-end. Inspection of the terminal 15 nucleotides at either end revealed an almost identical sequence stretch of eight nucleotides (Fig. 2C, boxed sequences). Apparently, only one of these boxes can be removed at a time. This may either indicate the presence of an essential higher order RNA

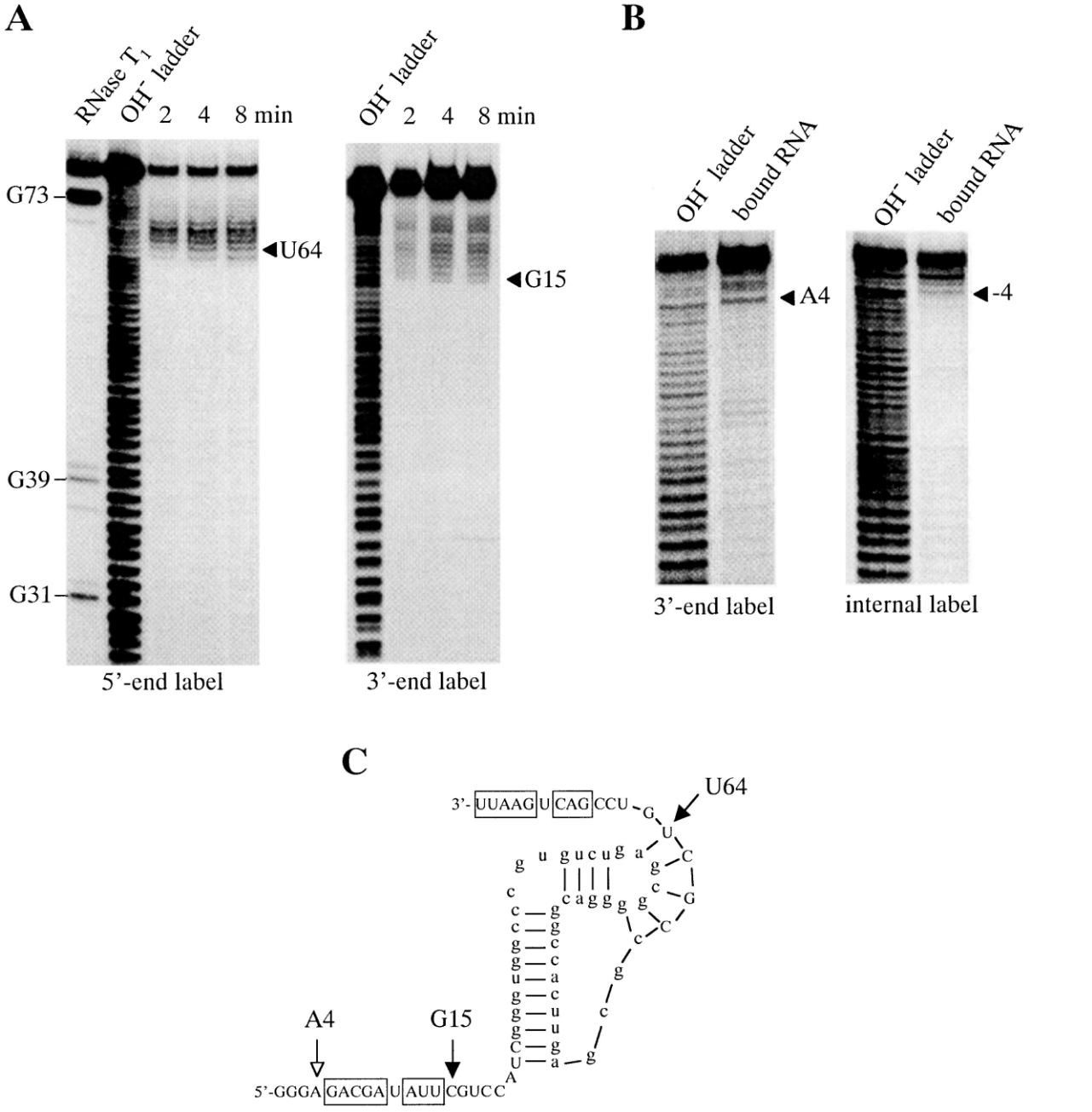

Figure 2. Determination of a minimal binding core of aptamer 2-16. (A) Alkaline hydrolysis ladders of 5′ and 3′ (^{32}P)-labelled 2-16 RNA were incubated with MITat 1.4 cells at 0 °C and aliquots were taken after 2, 4 and 8 min. Those aptamer variants that were able to bind to trypanosomes were separated from unbound RNA variants by centrifugation and analysed on denaturing polyacrylamide gels. Arrowheads point to the 3′-boundary at U64 and the 5′-boundary at G15. (B) Boundary determination with aptamer 2-16/67 lacking 10 nucleotides from the 3′-end. Left: 3′-end labelled 2-16/67 RNA. Right: internally [α-^{32}P] UTP labelled RNA. The arrowheads point to the 5′-boundary at A4 and to the shortest aptamer variant that was still active in binding. (**C**) Secondary structure model of aptamer 2-16. Arrows indicate the 5′- and 3′-boundaries. The open arrow at position A4 denotes the boundary as determined with aptamer 2-16/67. Boxes indicate a 9-nucleotide sequence containing eight identical bases within the two primer binding sites (indicated by capital letters).

interaction or a direct interaction of this sequence with the target during the binding reaction.

We further tested the stability of the 3′-shortened aptamer 2-16/67 after binding to MITat 1.4 trypanosomes. Internally [α-^{32}P] UTP labelled RNA was incubated with living parasites at 0 °C for 20 min. The cells were washed to remove unbound RNA and further incubated at 24 °C. After 20 min, significant amounts of the full length aptamer were still present (Fig. 3A). The half life of 2-16/67 aptamer was determined to be 17 min (Fig. 3B) which demonstrates a 3–5 fold higher stability in comparison to the parental 2-16 RNA (compare with Fig. 1B). In addition, the experiment in Fig. 3A demonstrates that the RNA is not degraded to small hydrolytic fragments. The major degradation products have a length of 50–60 nt which accumulate over time (Fig. 3B). This is suggestive of a minimal RNA binding core of about 50 nt that is resistant to cellular RNases.

Cellular fate of trypanosome-bound aptamers

To visualise the fate of aptamer 2-16 after binding to its target within the flagellar pocket, we performed in situ fluorescence microscopy. A 5′-fluorophore conjugated 2-16 RNA preparation was used to follow the localisation of the fluorescence signal at 0 °C as well as at 37 °C (Fig. 4). At 0 °C, a punctate fluorescence signal (red) next to the kinetoplast (blue) was detected (Fig. 4a). However, upon shifting the temperature to 37 °C, endocytosis of the aptamer occurs. Figures 4b–d show representative pictures of the different stages of the uptake process. At an early stage (2–5 min), the fluorescence signals appeared in the FP as well as in numerous vesicles between the kinetoplast and the nucleus (Fig. 4b). After 10–30 min, fluorescence signals were detected in extended endosomal compartments (Fig. 4c) and a further incubation at 37 °C for 60–120 min led to the accumulation of the signal in a single large compartment close to the cell nucleus (Fig. 4d). As a marker for the different endocytotic compartments, we chose transferrin conjugated to the green fluorescent BODIPY FL fluorophore. Endocytosis of transferrin is known to be mediated by a heterodimeric receptor located within the flagellar pocket and the protein is transported in endosomal vesicles to the lysosome.[27,37] This uptake pathway was verified using fluorophore conjugated human transferrin (Fig. 4e–h) under the same conditions as for the uptake of aptamer 2–16. Comparison of Fig. 4a–4d with Fig. 4e–h indicates a similar route in both cases.

Co-localisation of RNA aptamers and transferrin

To investigate the possible co-localisation of RNA aptamer 2-16 with transferrin we performed double staining experiments with fluorescently labelled transferrin and 5′-BODIPY TMR-C_5-labelled 2-16 RNA. The two preparations were incubated with living trypanosomes at 0, 10, and 24 °C for 20 min and at 37° for 90 min. Figure 5 shows a representative result. At 0 °C both, 2-16 RNA and transferrin stained the flagellar pocket (Fig. 5a). The two fluorescence signals only overlapped in about 50% of the cases, which may indicate the existence of subdomains within the flagellar pocket. At 10 °C, endocytosis is initiated (Fig. 5b and e) and numerous vesicles containing both, RNA and transferrin, were identified. At 24 °C, both markers co-localise

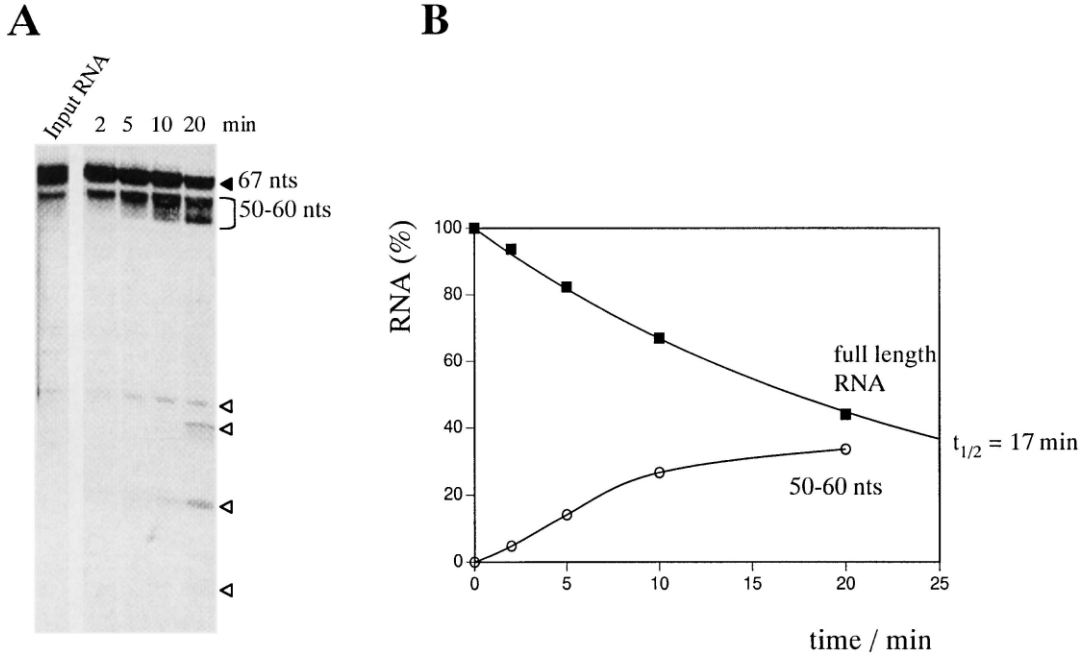

Figure 3. Degradation kinetic of 2-16/67 RNA bound to MITat 1.4 trypanosomes. (A) The RNA aptamer was incubated with parasites (2×10^8 cells/mL) for 20 min at 0 °C and the cells including cell-bound RNA were isolated and further incubated at 24 °C. The electrophoretic mobility of the full length 2-16/67 RNA (67 nt) and of the main degradation products (50–60 nt) are indicated on the right. Open triangles annotate minor hydrolysis products with a length of 5–15 nt. (B) Graphic representation of the degradation kinetic derived from a quantification of the band intensities in panel (A). Filled squares: degradation kinetic of aptamer 2-16/67. Open circles: accumulation of the 50–60 nt degradation products. The half-life ($t_{1/2}$) value was determined by exponential curve fitting.

in endosomal vesicles that cover a large area between the flagellar pocket and the nucleus (Fig. 5c and f). Inspection of $\geqslant 100$ cells in four independent experiments revealed that the majority of vesicles contained both labels although with varying intensities. In some cases, RNA-fluorescence was observed in extended, network-like compartments which likely represent collecting tubules as described by Webster[35] and Brickman et al.[36] Ultimately, after prolonged incubation at 37 °C, both labels were detected in the lysosome (Fig. 5d and g).

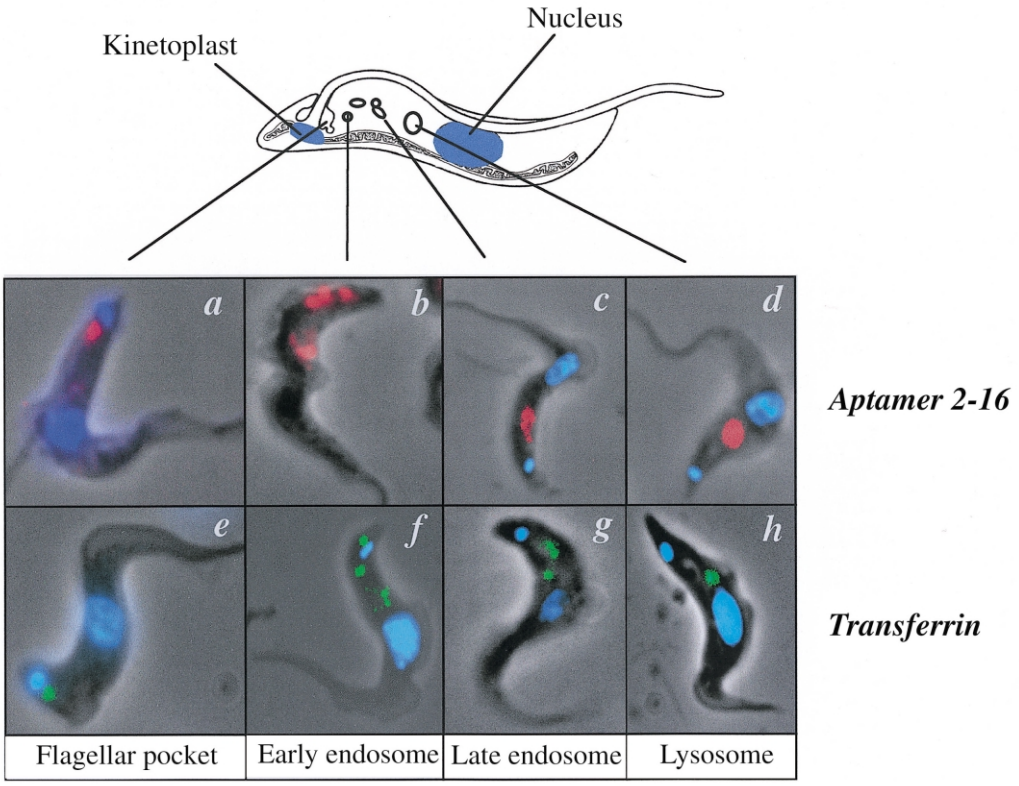

Figure 4. Fluorescence microscopy of trypanosome-bound RNA aptamer (red) and transferrin (green). The parasite cells are counter-stained with Hoechst H33342 to indicate the nucleus and the kinetoplast (blue). Top row, localisation of aptamer 2-16 at 0 °C (**a**) and after a temperature shift to 37 °C: (**b**) incubation at 37° for 2–5 min; (**c**), at 37° for 20 min and (**d**) at 37° for 120 min. The punctate red fluorescence at 0 °C indicates binding to the flagellar pocket (see line drawing on the top). Endosomal uptake and transport to the lysosome can be seen in **b**–**d**. Bottom row, receptor mediated endocytosis of transferrin as monitored by direct green fluorescence. At 0 °C, transferrin binds to its receptor located within the flagellar pocket (**e**). At 37 °C, the different stages of transport via endosomal compartments to the lysosome can be seen (**f**–**h**).

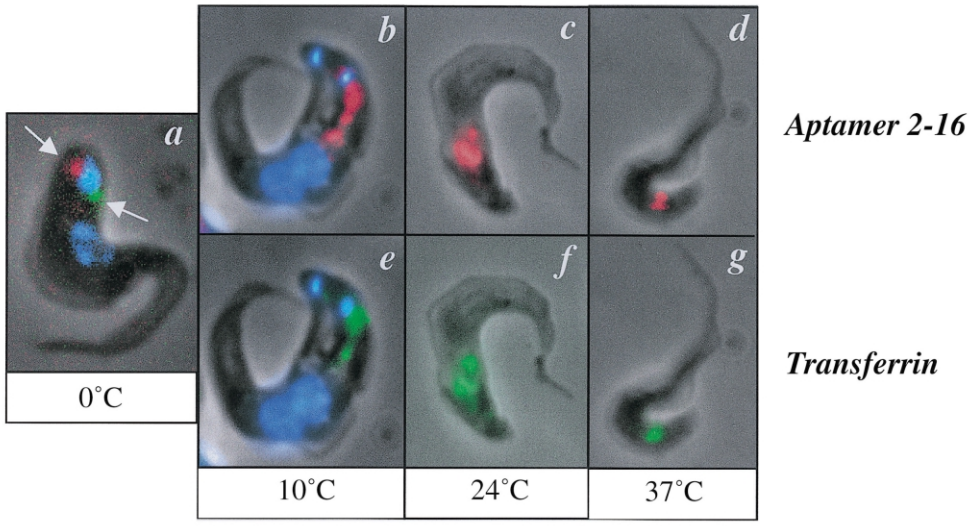

Figure 5. Co-localisation of fluorophore-conjugated aptamer 2–16 (red) and fluorescence-labelled transferrin (green). Trypanosomes were simultaneously incubated with RNA (100 nM) and transferrin (3 μM) at the indicated temperatures for 10–20 min (**a**–**c, e, f**) or for 120 min (**d**, **g**). At all stages of endocytosis and endosomal transport, similar staining patterns are observed.

Together, these results show that the uptake of aptamer 2-16 follows a similar, if not identical route as the receptor mediated endocytosis of transferrin and both molecules are ultimately transported to the lysosome.

Using aptamer 2-16 as a 'piggy-back' carrier

The above described cellular localisation experiments raised two issues: first, it was necessary to confirm that the detected fluorescence signals are due to the presence of fluorophore-coupled RNA and not to the fluorescence label alone. Second, based on the identified internalisation and transport pathway, we reasoned that aptamer 2–16 should be able to function as a carrier to transport aptamer-coupled compounds to the lysosome of the parasite. Both issues were addressed in a set of experiments where we performed indirect in situ fluorescence staining experiments with internally biotinylated aptamer preparations. As biotinylation substrate we used the tethered biotin-16-UTP nucleotide (biotin-ε-aminocaproyl-γ-aminobutyryl-[5-(3-aminoallyl)-uridine-5′-triphosphate). The modified UTP was co-transcriptionally incorporated into aptamer 2-16 with a stoichiometry of 1–2 biotin moieties per RNA (Fig. 6). After binding to live trypanosomes the biotin-conjugated RNAs were detected using a fluorophore-coupled anti-biotin antibody. Identical staining patterns as described above for the 5′ fluorophore-coupled aptamer preparations were observed (Fig. 6a–c). Biotin-modified aptamer RNA was identified within the flagellar pocket, in endosomal vesicles and inside of the lysosome. Thus, the data verify that aptamer 2–16 can be used as a 'piggy-back' carrier to internalise and transport aptamer-conjugated compounds to the lysosome of the trypanosome cell.

Discussion

In this study we demonstrate endocytosis and intracellular trafficking of RNA aptamers after binding to a

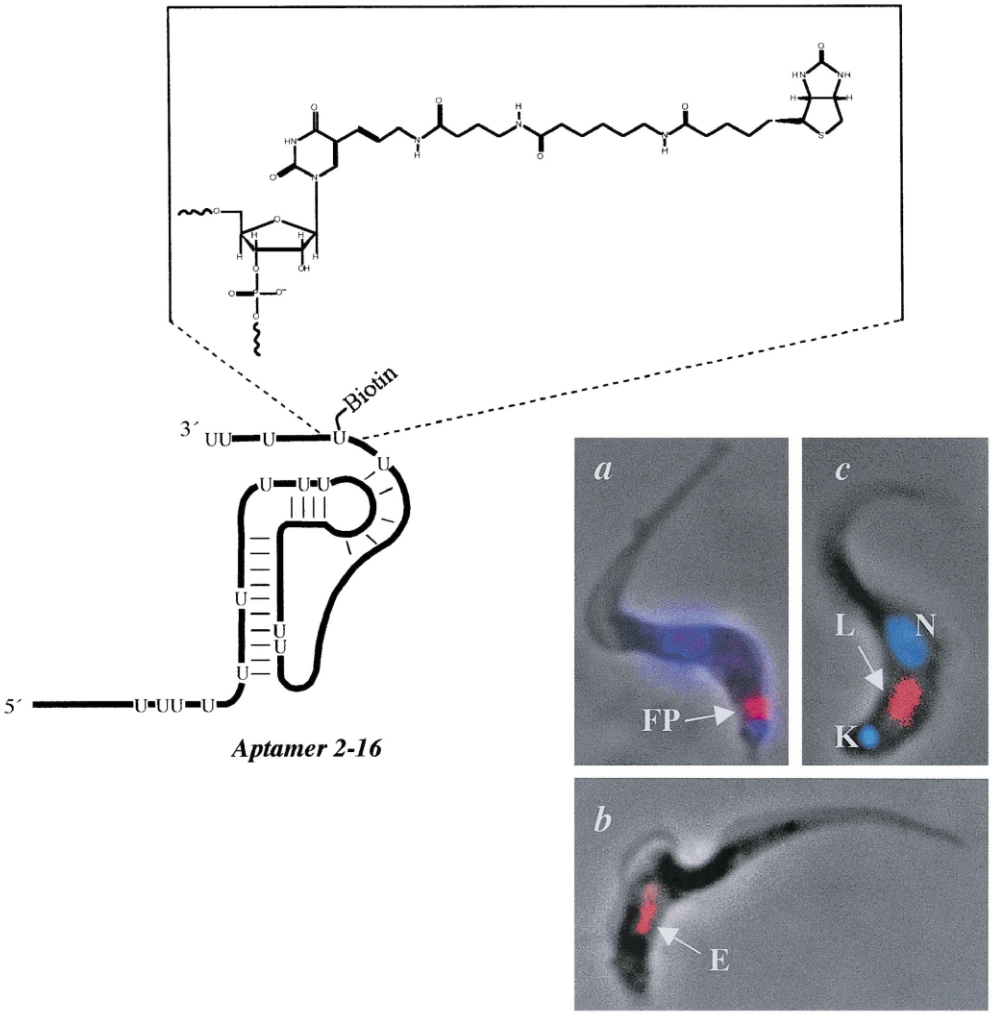

Figure 6. Targeting aptamer-conjugated biotin molecules to the lysosome. Uridylate residues within aptamer 2-16 were modified with an aminocaproyl-γ-aminobutyryl-[5-(3-aminoallyl)-tethered biotin side group (boxed insert). Reaction conditions were chosen to incorporate 1–2 biotin residues per RNA. Since aptamer 2-16 contains a total of 16 U-residues the reaction resulted in a population of modified RNAs with 1–2 biotin groups statistically distributed over the entire length of the aptamer. Only one example is depicted in the RNA secondary structure shown. After binding to live trypanosomes, a fluorophore-conjugated anti-biotin antibody detects the biotin label in (**a**) the flagellar pocket (FP), (**b**) within endosomal vesicles (E) and (**c**) within the lysosome (L). "K" indicates the position of the kinetoplast and the "N" the nucleus of the trypanosome cell.

specific protein target located within the flagellar pocket of African trypanosomes. The RNAs are ultimately transported to the lysosome and although being partly degraded during the process, we identified an RNA core sequence of about 50 nt with an increased stability towards cellular RNases. The endocytotic uptake of the RNAs is sequence specific and the aptamers co-localise with transferrin during all stages of the vesicular trafficking process.

Besides the regulated uptake of essential nutrients and macromolecules by receptor mediated endocytosis, trypanosomes also perform pinocytosis.[35,36] Several observations rule out the unspecific ingestion of the aptamers via fluid uptake. First, incubation of the parasites with a biotinylated pool of randomised RNA sequences gave no fluorescence signal. Second, the binding studies as well as the fluorescence localisation experiments were performed in the presence of a 1000-fold molar excess of yeast tRNA, and no competition of binding or reduced fluorescence intensities were detected. In addition, the results of the boundary experiments demonstrate a sequence specificity of the process. This observation is further strengthened by the result that the truncated aptamer 2-16/55 lost its binding activity and did not generate a fluorescence signal. Furthermore, all aptamers from our previous in vitro selection experiments[31] were tested for endocytotic uptake using biotinylated RNA preparations in combination with the fluorophore-conjugated anti-biotin antibody for detection. The differences in the binding efficiencies were qualitatively reflected in the intensities of the fluorescence signals: strong fluorescence signals were observed with strong binders and weak signals resulted from low affinity aptamers.

The co-localisation of transferrin and RNA during all stages of endocytosis may indicate identical receptor molecules in the flagellar pocket. We have previously shown that aptamer 2-16 can be cross-linked to a 42 kDa protein,[31] which corresponds to the molecular mass of ESAG 7, a subunit of the heterodimeric transferrin receptor in *T. brucei*.[28] However, in competition experiments, no interference of aptamer binding or fluorescence was detected in the presence of 3 μM transferrin. The binding affinity of bovine transferrin for the heterodimeric transferrin receptor was 2–3 μM in the case of MITat 1.4 trypanosomes,[38] with an estimated copy number of 2000–3000 molecules per cell. Human transferrin was shown to be endocytosed with an identical uptake kinetic,[38] and the dissociation constant was determined to 30 nM.[39] Thus, most of the receptor molecules are occupied at a transferrin concentration of 3 μM and the lack of competition either indicates a different protein target for the aptamer or different binding sites on the ESAG 7 receptor subunit.

Two enzyme activities involved in the nucleic acid metabolism in *T. brucei* may play a role in the binding and processing reactions of the RNA aptamers. Trypanosomatids are unable to perform the de novo synthesis of purines,[25,40] hence several purine nucleoside[41] as well as nucleobase[26] transporters catalyse the uptake of purines from the outer environment. In addition, several nuclease activities have been identified in *T. brucei* and other trypanosomatids. A 3′-nucleotidase/nuclease activity was found on the surface of *trypanosoma* species[42,43] as well as in *leishmania*[44] and *crithidia*.[45] In *Crithidia fasciculata* it was shown that the enzyme is upregulated 1000-fold under purine starvation conditions[45,46] indicating a functional relationship of such nucleases to purine metabolism. Degradation of RNA aptamers during the process of uptake and transport may be due to such RNase activities in the flagellar pocket as well as within the endosomal compartments. Furthermore, RNases as well as purine transporters could be candidates for the 42 kDa protein binding target. However, a general affinity of these enzymes for RNA substrates is unlikely to be responsible for the binding of the aptamers. First, yeast tRNA is unable to inhibit either aptamer binding or uptake even at 10^4 fold higher concentrations. Second, the boundary experiments show a clear sequence/structure specificity of the interaction. In addition, neither randomised RNA sequences nor the 2–16-derived aptamer 2-16/55 are binding to or endocytosed by *T. brucei* cells.

Conclusion

Together, these data show that aptamers can be used to transport RNA-conjugated compounds to intracellular compartments in African trypanosomes. Specifically, RNA aptamer 2-16 is capable of targeting the lysosome of the parasite. This strategy has its precedence in the natural resistance of humans towards infections with the cattle pathogen *T. brucei brucei*.[29,47] Human serum contains several lytic factors (TLFs), which are components of the high density lipoprotein (HDL) fraction. TLFs are taken up by receptor mediated internalisation of HDL and are transported to the lysosome. Within the lysosome the TLFs become activated leading to lysosomal lysis and as a consequence to the self-destruction of the parasite. Analogously, aptamer 2-16 can be used to 'piggy back' RNA-coupled toxins to the lysosome, which represents a novel therapeutic strategy to inhibit the growth of the parasite.

Experimental

Trypanosomes

The bloodstream life cycle stage of *Trypanosoma brucei* 427-MITat serodeme, variant clones MITat 1.2 and MITat 1.4,[32] were grown in HMI-9 medium[33] supplemented with 10% (v/v) heat-inactivated bovine foetal calf serum.[34]

In vitro transcription, radioactive RNA labelling and RNA biotinylation

RNAs were transcribed either from PCR-generated DNA templates or from linearised plasmids.[31] In vitro transcription reactions were performed in 40 mM Tris/

HCl pH 8, 12 mM $MgCl_2$, 5 mM DTT, 2 mM spermidin and 0.002 % (v/v) Triton X-100. The reactions further contained 1 mM of each NTP, 0.4 U/mL T7 RNA polymerase and 1–10 pmol DNA template. Incubations (2 h, 37 °C) were stopped by the addition of DNase I (40 U). Aptamers were biotinylated as described[31] using 5–50 μM biotin-16-UTP (Roche Diagnostics) in the in vitro transcription mix. Similarly, internally labelled RNAs were transcribed in the presence of [α-^{32}P] UTP.[31] The 5′-end labelling of RNA was performed with 1–10 μg dephosphorylated RNA, T4 polynucleotide kinase and [γ-^{32}P] ATP (20 μCi) according to standard procedures. The 3′-end labelling of RNA (1–10 μg) was performed in 50 mM Tris/HCl pH 8, 10 mM $MgCl_2$, 10 mM DTT, 10 % (v/v) DMSO and 1 mM ATP, using 20 μCi [^{32}P]-pCp and 10 U RNA ligase. Incubation was for 30 min at 20 °C followed by 15 min at 37 °C. All labelled RNA products were purified from unincorporated label by gel filtration.

Construction of truncated RNA aptamers

The double stranded DNA template for the transcription of aptamer 2-16 shortened by 14 nucleotides at the 5′-end and 10 nucleotides at the 3′-end (RNA 2-16/55) was synthesised by PCR using the template oligodeoxynucleotide: 5′-GTCCATCGGGTGGCCCGTGTCT GAGCGGGGACGGCCACTTGAGCGCCGCTGTC GA-3′ and primers: 5′-GCGAAGCTTTAATACGAC TCACTATAGGGTCCATCGGGTGGCCCGTGTC-3′ and 5′-GCAGTCGACAGCGGCGCTCAAGTGG-3′. The PCR products were digested with *Hin*d III and *Sal* I and cloned into pUC118. Dideoxy terminator sequencing of both strands confirmed the correct sequence. The resulting plasmid was linearised with *Hin*d II for run-off transcription as described above. The double stranded DNA template for the transcription of aptamer 2-16/67 was generated by PCR using a plasmid encoded full length 2-16 RNA gene[31] and primers 5′-GCGAAGCTTTAATACGACTCACTATAGGGAG ACGATATTCGTCCATC-3′ and 5′-GCAGTCGACA GCGGCGCTCAAGTGG-3′. The PCR product was cleaved with *Hin*d II for run-off transcription.

Boundary determination

Radiolabelled RNA aptamer 2-16 (0.5 μM) was subjected to alkaline hydrolysis in 0.5 M $NaHCO_3$ for 14 min at 95 °C. The solution was cooled to 0 °C and loaded onto a Sephadex G50 gel filtration column. The eluate was precipitated with ethanol, the RNA pellet briefly air-dried and dissolved in PBSG binding buffer (20 mM $Na_xH_yPO_4$ pH 7.4, 130 mM NaCl, 5 mM KCl, 2 mM $MgCl_2$, 20 mM glucose and 0.2 mM β-mercaptoethanol). The pool of shortened RNA variants was incubated with *T. brucei* cells (2×10^8 cells/mL) in PBSG containing 100 nM yeast tRNA at 0 °C for 20 min. Bound RNA was separated from unbound RNA by three washes in 1 mL ice-cold PBSG containing BSA (100 nM) and yeast tRNA (100 nM). Bound RNA was collected together with the parasite cells and re-isolated by phenol extraction and ethanol precipitation. RNA samples were loaded onto a 12% (w/v) denaturing polyacrylamide gel. Dried gels were analysed by autoradiography.

K_d measurements

Uniformly ^{32}P-labeled aptamer 2-16 and its shortened derivatives (0.2–400 nM) were incubated with living trypanosomes ($1–3\times10^8$ cells/mL) in PBSG buffer containing 100 nM yeast tRNA for 30 min at 0 °C. After three washes with 1 mL PBSG, the percentage of bound RNA was determined by scintillation counting. K_d values were derived from a Scatchard analysis of the binding data with the slope of the plot representing $-1/K_d$.[31]

Determination of RNA stability

Uniformly ^{32}P-labelled RNA (1 nM) or 5′-end labelled aptamers (5–10 nM) were incubated with *T. brucei* cells in PBSG at cell densities of 3×10^8/mL for 20 min at 0 °C. Bound RNA was separated from unbound RNA by three washes with 1 mL PBSG (0 °C). The cells including bound aptamer RNAs were resuspended in PBSG and further incubated at 0, 12, 24 and 37 °C for up to 40 min. At various time points, aliquots were taken and immediately diluted with ice-cold gel loading buffer (50 mM Tris/HCl pH 8, 2 mM Na_2EDTA, 0.05 % (w/v) SDS, 8 M urea). Samples were heated to 95 °C for 5 min and analysed on denaturing 12 % (w/v) polyacrylamide gels. Dried gels were exposed to X-ray films and autoradiographs were analysed by densitometry. For each time point, the fraction of full length RNA was determined relative to the input RNA. Aptamer half-lifes ($t_{1/2}$) were determined graphically or by exponential curve fitting.

In situ fluorescence

Bloodstream stage trypanosomes were harvested at a cell density of 2×10^6 cells/mL, washed in PBSG (4×) and pre-incubated in PBSG for 30 min at 20 °C. Human transferrin coupled to the green fluorescent BODIPY FL dye (Molecular Probes) was used to track the endocytotic pathway. The transferrin-BODIPY conjugate was incubated at a concentration of 3–5 μM with *T. brucei* cells (1×10^8/mL) at 0 °C for 15 min. The cells were washed (2×) with ice-cold PBSG and either kept on ice to stain the flagellar pocket or shifted to 37 °C to initiate endocytosis. At various time points, parasite cells were collected by centrifugation, smeared onto microscopic slides, briefly air-dried and mounted in ProLong Antifade (Molecular Probes). Slides were examined as described.[31] For the in situ fluorescence localisation of RNA, 5′-BODIPY TMR-C_5–labelled RNA aptamers[31] (10 ng/μL) were incubated with trypanosomes and processed as described above. Nuclear and kinetoplast DNA were stained with Hoechst H-33342 (Molecular Probes). For the indirect fluorescence analyses, biotinylated RNA aptamers were incubated with trypanosomes at 0 °C. The RNA was detected by the addition of a 1:100 dilution of a monoclonal Cy™3-conjugated anti-biotin antibody (Dianova). To determine the vesicular distribution of the RNA aptamers, incubation was performed at temperatures ranging from 12 to 37 °C.

Acknowledgements

The authors are grateful to U. Müller for discussion, graphical work and input in the quantification of the kinetic data. We further thank M. Brecht and U. Müller for critically reading the manuscript and F. Melchior for providing access to her digital imaging facility. The work was supported in part by grants from the Deutsche Forschungsgemeinschaft (DFG) and the International Research Scholar Program of the Howard Hughes Medical Institute (HHMI) to H.U.G.

References

1. Anderson, R. M. *Int. J. Parasitol.* **1998**, *28*, 551.
2. Lanzer, M.; Gross, U.; Moll, H. *Parasitol. Today* **1997**, *13*, 18.
3. Newbold, C. I. *Curr. Opp. Microbiol.* **1999**, *2*, 420.
4. Bogdan, B.; Röllinghoff, M. *Int. J. Parasitol.* **1998**, *28*, 121.
5. Donelson, J. E.; Hill, K. L.; El-Sayed, N. M.A. *Mol. Biochem. Parasitol.* **1998**, *91*, 51.
6. Ramasamy, R. *Biochim. Biophys. Acta* **1998**, *1406*, 10.
7. Bogdan, B.; Röllinghoff, M. *Parasitol. Today* **1999**, *15*, 22.
8. Burleigh, B. A.; Andrews, N. W. *Curr. Opp. Microbiol.* **1998**, *1*, 461.
9. Preiser, P. R.; Jarra, W.; Capiod, T.; Snounous, G. *Nature* **1999**, *398*, 618.
10. Sternberg, J. M. *Chem. Immunol.* **1998**, *70*, 186.
11. Cross, G. A. M. *Bioessays* **1996**, *18*, 283.
12. Rudenko, G.; Cross, M.; Borst, P. *Trends Microbiol.* **1998**, *6*, 113.
13. Borst, P.; Bitter, W.; Blundell, P. A.; Chaves, I.; Cross, M.; Gerrots, H.; van Leeuwen, F.; McCulloch, R.; Taylor, M.; Rudenko, G. *Mol. Biochem. Parasitol.* **1998**, *91*, 67.
14. Lamont, G. S.; Tucker, R. S.; Cross, G. A. M. *Parasitology* **1986**, *92*, 355.
15. Turner, C. M.; Barry, J. D. *Parasitology* **1989**, *99*, 67.
16. Turner, C. M. R. *FEMS Microbiol. Lett.* **1997**, *153*, 227.
17. Carrington, M.; Miller, N.; Blum, M.; Roditi, I.; Wiley, D.; Turner, M. *J. Mol. Biol.* **1991**, *221*, 823.
18. Blum, M. L.; Down, J. A.; Gurnett, A. M.; Carrington, M.; Turner, M. J.; Wiley, D. C. *Nature* **1991**, *362*, 603.
19. Carrington, M.; Boothroyd, J. *Mol. Biochem. Parasitol* **1996**, *81*, 119.
20. Borst, P.; Fairlamb, A. H. *Annu. Rev. Microbiol.* **1998**, *52*, 745.
21. Pays, E.; Nolan, D. P. *Mol. Biochem. Parasitol.* **1998**, *91*, 3.
22. Seyfang, A.; Duszenko, M. *Eur. J. Biochem.* **1993**, *214*, 593.
23. Balber, A. E. *Crit. Rev. Immunol.* **1990**, *10*, 177.
24. Overath, P.; Stierhof, Y.-D.; Wiese, M. *Trends Cell Biol.* **1997**, *7*, 27.
25. Cohn, C. S.; Gottlieb, M. *Parasitol. Today* **1997**, *13*, 231.
26. de Koning, H. P.; Jarvis, S. M. *Mol. Biochem. Parasitol.* **1997**, *89*, 245.
27. Salmon, D.; Geuskens, M.; Hanocq, F.; Hanocq-Quertier, J.; Nolan, D.; Ruben, L.; Pays, E. *Cell* **1994**, *78*, 75.
28. Steverding, D.; Stierhof, Y.-D.; Chaudri, M.; Ligtenberg, M.; Schell, D.; Beck-Sickinger, A. G.; Overath, P. *Eur. J. Cell Biol.* **1994**, *64*, 78.
29. Hajduk, S. L.; Hager, K. M.; Esko, J. D. *Annu. Rev. Microbiol.* **1994**, *48*, 139.
30. Coppens, I.; Bastin, P.; Courtoy, P. J.; Baudhuin, P.; Opperdoes, F. R. *Biochem. Biophys, Res. Commun.* **1991**, *178*, 185.
31. Homann, M.; Göringer, H. U. *Nucleic Acids Res.* **1999**, *27*, 2006.
32. Cross, G. A. M. *Parasitology* **1975**, *71*, 393.
33. Hirumi, H.; Hirumi, K. *Parasitol. Today* **1994**, *10*, 80.
34. Brun, R.; Schönenberger, M. *Acta Trop.* **1979**, *36*, 289.
35. Webster, P. *Eur. J. Cell Biol.* **1989**, *49*, 295.
36. Brickman, M. J.; Cook, J. M.; Balber, E. B. *J. Cell Science* **1995**, *108*, 3611.
37. Grab, D. J.; Wells, C. W.; Shaw, M. K.; Webster, P.; Russo, D. C. *Eur. J. Cell Biol.* **1992**, *59*, 398.
38. Steverding, D.; Stierhof, Y.-D.; Fuchs, H.; Tauber, R.; Overath, P. *J. Cell Biol.* **1995**, *131*, 1173.
39. Bitter, W.; Gerrits, H.; Kieft, R.; Borst, P. *Nature* **1998**, *391*, 499.
40. Hammond, D. J.; Gutteridge, W. E. *Mol. Biochem. Parasitol.* **1988**, *13*, 243.
41. Carter, N. S.; Fairlamb, A. H. *Nature* **1993**, *361*, 173.
42. Gbenle, G. O.; Opperdoes, F. R.; Van Roy, J. *Acta Trop.* **1986**, *43*, 295.
43. Gottlieb, M.; Gardiner, P. R.; Dwyer, D. M. *Comp. Biochem. Physiol. B.* **1986**, *83*, 63.
44. Debrabant, A.; Gottlieb, M.; Dwyer, D. M. *Mol. Biochem. Parasitol.* **1995**, *71*, 51.
45. Gottlieb, M. *Science* **1985**, *227*, 72.
46. Yamage, M.; Debrabant, A.; Dwyer, D. M. *J. Biol. Chem.* **2000**, in press.
47. Hager, K. M.; Hajduk, S. L. *Nature* **1997**, *385*, 823.